GA–A27685

THE GENERAL ATOMICS FUSION THEORY

FINAL REPORT TO THE U.S. DEPARTMENT OF ENERGY

FOR THE PERIOD OF JANUARY 15, 2011 THROUGH JANUARY 14, 2014

by
PROJECT STAFF

DATE PUBLISHED: DECEMBER 2013

GENERAL ATOMICS

DISCLAIMER

GA–A27685

THE GENERAL ATOMICS FUSION THEORY

FINAL REPORT TO THE U.S. DEPARTMENT OF ENERGY

FOR THE PERIOD OF JANUARY 15, 2011 THROUGH JANUARY 14, 2014

by
PROJECT STAFF

Work supported by
U.S. Department of Energy
under Grant No. DE-FG02-95ER54309

GENERAL ATOMICS PROJECT 03726
DATE PUBLISHED: DECEMBER 2013

GENERAL ATOMICS

ABSTRACT

The objective of the fusion theory program at General Atomics (GA) is to significantly advance our scientific understanding of the physics of fusion plasmas and to support the DIII–D and other tokamak experiments as well as ITER research activities. The program plan is aimed at contributing significantly to the Fusion Energy Science, the Tokamak Concept Improvement, and ITER goals of the Office of Fusion Energy Sciences (OFES). Significant progress was made in each of the important areas of our research program during the last grant period GY11-13. This includes development of a new formulation of 3D local equilibrium for use with solving the neoclassical equations in 3D geometry; continued validation of the EPED pedestal height and width model and its application to develop a new working model for RMP ELM suppression and tested it against DIII-D data; validation of M3D-C1 plasma response against DIII-D edge measurements and its extensive applications to model DIII-D RMP experiments; completion of M3D-C1 and NIMROD linear ELM benchmarking calculations including self-consistent diamagnetic stabilization effect; demonstration that non-linear M3D-C1 calculations of DIII-D plasma response were generally in good agreement with the linear calculations; demonstration with NIMROD simulations of a DIII-D MPI discharge that measurable differences should be observed in the timing and amplitude of the radiated power when n=1 fields are applied during the thermal quench; demonstration with analysis of density data from a recent DIII-D MGI experiment with n = 1 RMP fields that impurity mixing varies significantly with the n = 1 mode phase as would be expected from the NIMROD predictions; proposed a new composite pellet for DIII-D and ITER that may fully ablate in the hot plasma without hitting the far wall; performed first transport analysis of an ELM-suppressed DIII-D discharge using the quasi-linear transport code RMPtran with M3D-C1 RMP plasma response; exploration of the accuracy and limitations of the Sauter bootstrap-current model using the drift-kinetic neoclassical code NEO; successful completion of a transport analysis of a DIII-D double-barrier QH-mode discharge for all transport channels using TGLF, NEO, and the new spectral-shift paradigm; re-engineered the OpenMP implementation in GYRO; development of a new 4D reduced cyclokinetic code rCYCLO to test 3D gyrokinetic simulations; initiated development of a new method for solution of the Fokker-Planck-Landau equation based on a Gaussian radial basis function expansion; updated GYRO to accommodate a kinetic species with an isotropic slowing-down distribution; and development of a new Python-based integrated modeling framework OMFIT with recent updates focusing on kinetic EFIT reconstructions, transport modeling, and edge stability analysis.

TABLE OF CONTENTS

1. HIGHLIGHTS OF THEORY WORK IN GY11–13

During the past 3 years, significant progress was made in each of the important areas of our research program:

- Enhancements to EFIT including a new capability to reconstruct equilibria with ion-temperature measurements as additional internal flux-surface constraints that can be used to improve the inboard and outboard ion-temperature overlapping.
- Development of a new formulation of 3D local equilibrium for use with solving the neoclassical equations in 3D geometry that is a true generalization of the Miller 2D local-equilibrium method for non-axisymmetric plasma configurations with nested flux-surfaces.
- Continued validation of the EPED pedestal height and width model against DIII-D and other tokamak data and its application to develop a new working model for RMP ELM suppression in which the penetrated perturbation field stops the inward propagation of the edge barrier and tested it against DIII-D discharges.
- Completed an analysis of a broad database of DIII-D RMP ELM-suppressed discharges which consistently finds that the ELM-suppressed discharges are stable to peeling-ballooning modes, and in the absence of RMPs the discharges approach the peeling-ballooning instability boundary and ELMs are observed.
- Demonstred with a study of ballooning criticality near the separatrix in model equilibria based on DIII-D, JET, C-Mod and ITER that ballooning physics might lead to wider scrape-off layer widths on ITER.
- Demonstration with an initial study of the pedestal structure in more than 300 JET discharges with the new ITER-like-wall (ILW) that the EPED predicted pedestal heights in ILW discharges have similar (~20%) accuracy as earlier JET carbon-wall discharges.
- Validation of M3D-C1 plasma response against DIII-D edge measurements and its extensive applications to model DIII-D RMP experiments with interesting results including a potential island opening mechanism for constraining the pedestal width in RMP ELM suppression.
- Completion of M3D-C1 and NIMROD linear ELM benchmarking calculations which shows that the growth rates obtained are in good agreement with each other, and in the particular case studied the self-consistent diamagnetic stabilization effect was stronger than that implied by a high-n limit formula.
- Much improved agreement among the predictions of the linearized plasma response by the MARS-F, M3D-C1, and IPEC MHD codes through a careful analysis of the

way in which the external perturbation phase and amplitude are implemented in these codes.

- Demonstration that non-linear M3D-C1 calculations of DIII-D plasma response to applied 3D fields were generally in good agreement with the linear calculations for cases where the linear approximation was expected to remain valid.
- Implementation of a capability to include a resistive wall of arbitrary thickness and axisymmetric geometry in M3D-C1 by treating it as a separate region in the computational domain.
- Demonstration with NIMROD simulations of a DIII-D MGI discharge that measurable differences should be observed in the timing and amplitude of the radiated power when n=1 fields are applied to influence the phase of the unstable 1/1 mode during the thermal quench.
- Indication from NIMROD simulations of massive gas injection in DIII-D that toroidally localized sources de-confine runaway electrons earlier in time consistent with an earlier growth of the n = 1 mode and that high-field side injection is especially effective at de-confining runaway electrons.
- Demonstration with analysis of density data from a recent DIII-D MGI experiment with n = 1 RMP fields to test NIMROD predictions that impurity mixing varies significantly with the n = 1 mode phase and that impurity mixes more efficiently into the core for the phases at which this would be expected from the NIMROD predictions.
- Development of a new MARS version with public based F90 FFT routines.
- Investigation of a method to produce a collimated stream of small pellets for disruption mitigation in ITER based on spallation of a large solid deuterium pellet into daughter fragments upon impact with a rigid surface.
- Proposed a new composite pellet for DIII-D and ITER with a boron or beryllium pellet core coated with a thin outer layer of lithium to prevent excessive cooling near the q = 2 surface that allows the pellet to fully ablate in the hot plasma without hitting the far wall.
- Modified and interfaced the Fokker-Planck code CQL3D with NIMROD to self-consistently investigate kinetic effects of runaway electrons under non-axisymmetric magnetic perturbations in tokamaks.
- Performed first transport analysis of an ELM-suppressed DIII-D discharge using the quasi-linear transport code RMPtran with M3D-C1 RMP plasma response which shows that RMP induces a large edge $E \times B$ particle transport with the induced core rotation braking Maxwell stress largely cancelled by the Reynolds stress, that may

explain the RMP density pump-out with little change in core rotation often observed in DIII-D RMP experiments.

- Improvements and applications of ORBIT-RF to simulate DIII-D fast-wave (FW) experiments including a demonstration with ORBIT-RF/AORSA simulations of DIII-D high-harmonic FW experiments that the synergistic effect observed in the DIII-D two-frequency FW heating experiments is due to coupling of the two harmonics by finite drift orbits.
- Exploration of the accuracy and limitations of the Sauter bootstrap-current model for a range of experimental DIII-D discharges using the drift-kinetic neoclassical code NEO which show that the Sauter model over-estimates the bootstrap current at low collisionality and largely under-estimates the bootstrap current at high collisionality.
- Successful completion of a transport analysis of a DIII-D double-barrier QH-mode discharge that had a nearly stationary ITB with XPTOR for all transport channels using TGLF, NEO, and the new spectral-shift paradigm for $E \times B$ shear suppression with very good agreement between the predicted and measured profiles.
- Reached an agreement to allow for the usage of the GACODE suite of analysis and simulations codes at JET that includes GYRO, NEO, and TGYRO.
- Re-engineered the OpenMP implementation in GYRO that significantly improves its parallel computation efficiency.
- Initiated development of a radically new method for solution of the 6D Fokker-Planck-Landau equation based on a Gaussian radial basis function expansion that may provide a closure-free alternative to MHD and a realistic method to solve the kinetic equation in the vicinity of the separatrix.
- Development of a new 4D reduced cyclokinetic code rCYCLO to test 3D gyrokinetic simulations based on the reduced cyclokinetic model recently developed.
- Performed preliminary nonlinear cyclokinetic (CK) simulations at low and high turbulence levels and at low and high ion-cyclotron frequencies using rCLYCLO that indicates CK transport is lower than transport from the corresponding gyrokinetic simulations.
- Updated GYRO to accommodate a kinetic species with an isotropic slowing-down distribution to improve the accuracy of the Alfvén-eigenmode stiff transport model for energetic-particle profile prediction.
- Development of the IMFIT Python-based integrated modeling tool to support tokamak data analysis and modeling and more recently a new OMFIT framework that facilitates efficient interactions among modules by treating files, data, and scripts as a

collection of objects in a MDSPlus-like tree structure with recent updates focusing on kinetic EFIT reconstructions, transport modeling, and edge stability analysis.

- Improvements to the ONETWO transport code including a recent version with enhancements to speed up both the RF calls and the P-NFREYA execution time and a significant expansion of the ONETWO plasma state file to accommodate new physics output.

As a consequence of these results, scientists from the Theory Group were selected to give a number of invited talks and colloquia as highlighted in the next section. Sections 3–5 provide more detailed descriptions of the advances and achievements made in each of the major areas. A list of publications is given in Section 6.

2. SIGNIFICANT PRESENTATIONS IN GY11–13

2013 PRESENTATIONS

55th APS DPP meeting in Denver, CO November 11–15, 2013:

- E.M. Bass gives an invited presentation "Predictions of the Transport-Limited Fusion Alpha Profile in ITER."
- E. Belli gives an invited presentation "Neoclassical Flows, Bootstrap Current, and Non-Axisymmetric Effects in the Tokamak Plasma Edge."
- G.M. Staebler gives an invited presentation "Predicting Internal Transport Barriers with the TGLF Transport mode."

23RD International Toki Conference, in Toki, Japan November 18-21, 2013:

- P.B. Snyder gives an invited presentation "Understanding the Physics of the H-Mode Pedestal and ELMs in Tokamaks."

International Sherwood Fusion Theory Conference in Santa Fe, NM April 15–17, 2013:

- E.A. Belli gave an oral presentation "Neoclassical Flows and Transport in the Tokamak Plasma Edge and Extensions to Include Non-Axisymmetric Effects."

Department of Energy Technical Program Review in Rockville, MD March 19, 2013:

- J. Candy gave a presentation "Computing and Storage Requirements for Fusion Energy Science."

US-EU Joint Transport Task Force Workshop in Santa Rosa, CA April 9–12 2013:

- J. Candy gave a presentation "Turbulent Energy Exchange: Calculation and Relevance for Profile Prediction."
- P.B. Snyder gave a presentation "Predicting and Optimizing the Pedestal Structure in Existing and Future Devices."
- G.M. Staebler gave a presentation "Predicting Transport Barriers with the TGLF Model."

10th ITPA Pedestal Meeting in Garching, Germany April 22-24, 2013:

- P.B. Snyder gave a presentation "Update on the EPED Model and Predictions for ITER."

IAEA Technical Meeting on Energetic Particles in Beijing, China September 17-20, 2013:

- R.E. Waltz gave a presentation "Prediction of the Fusion Alpha Density Profile from Local Marginal Stability to Alfven Eigenmodes in ITER."

2012 PRESENTATIONS

24TH IAEA Fusion Energy Conference in San Diego, USA October 8-13, 2012:

- E.M. Bass gave a presentation "Fully Gyro-Kinetic Modeling of Beam-Driven Alfven Eigenmodes in DIII-D Using GYRO."
- N.M. Ferraro gave a presentation "Edge Plasma Response to Non-Axisymmetric Fields in Tokamaks."
- V.A. Izzo gave a presentation "Impurity Mixing in Massive-Gas-Injection Simulations of DIII-D."
- P.B. Snyder gave a presentation "The EPED Pedestal Model: Extensions, Application to ELM-Suppressed Regimes, and ITER Predictions."
- G.M. Staebler gave an oral presentation "A New paradigm for E×B Velocity Shear Suppression of Gyro-Kinetic Turbulence and the Momentum Pinch."

54TH APS DPP meeting in Providence, Rhode Island October 29–November 2, 2012:

- J. Candy gave an invited tutorial presentation "Theory, Verification and Validation of Finite-Beta Gyro-Kinetics."
- V.A. Izzo gave an invited presentation "Impurity Mixing, Radiation Asymmetry, and Runaway Electron Confinement in MGI Simulations of DIII-D and ITER."
- A.D. Turnbull gave an invited presentation "Comparisons of Linear and Nonlinear Plasma Response Models for Non-Axisymmetric Perturbations."
- R.E. Waltz gave an invited presentation "Search for the Missing L-Mode Edge Transport and Possible Breakdown of Gyro-Kinetics."

18TH International Stellarator Workshop in Canberra, Australia January 29-February 3 2012:

- A.D. Turnbull gave a presentation "Comparison of Plasma Response Models for Non-axisymmetric Perturbations."

USBPO Disruption Mitigation Workshop in San Diego, California March 12-13 2012:

- V. Izzo gave a presentation "Disruption Mitigation Modeling Work."

APS-Sherwood Meeting in Atlanta, Georgia March 31 – April 3, 2012:

- R.E. Waltz gave an invited presentation "Gyro-Kinetic Simulations with External Resonant Magnetic Perturbations: Island Torque and Non-Ambipolar Transport with Rotation."

ITPA Pedestal Topical Meeting Hefei, China April 2-4, 2012:

- P.B. Snyder gave a presentation "An EPED-Based Working Model for RMP ELM Suppression" and a summary presentation "Discussion of Progress and Work Plan for ITER Urgent Issues in Pedestal Structure."

US Transport Task Force Workshop in Annapolis, MD April 10-13, 2012:

- P.B. Snyder gave a presentation "Developing and Testing the EPED Model for the 2011 JRT on Pedestal Structure."

39TH EPS Conference on Plasmas Physics in Stockholm, Sweden July 2-6, 2012:

- M. Choi gave a presentation "Modeling of Large-Orbit Fast-on Distribution Evolution with Multiple Frequency FW Heating."

EFTSOMP Workshop in Stockholm, Sweden July 9-10, 2012:

- R.E. Waltz gave an invited talk on ""Gyro-Kinetic Simulations with External Resonant Magnetic Perturbations: Island Torque and Non-Ambipolar Transport with Rotation."

6TH US-PRC Magnetic Fusion Collaboration Workshop in San Diego, California July 10-12, 2012:

- O. Meneghini gave a presentation "OMFIT: A New Approach to Integrated Modeling."

Magnetic Fusion Theory and Simulation Workshop in Hefei, China July 16–17, 2012:

- L.L. Lao gave a presentation "Recent Progress in Theory and Modeling of DIII-D Experiments."

International School of Plasma Physics in Varenna, Italy August 27-31, 2012:

- N.M. Ferraro gave a presentation "Modeling Edge Plasma Response to Non-Axisymmetric Magnetic Fields in Tokamaks."

EU Transport Task Force Workshop in Padua, Italy September 3-6, 2012:

- G.M. Staebler gave an invited presentation "Transport in the core-edge transition region."

ITPA MHD, Disruptions and Control Topical Meeting in San Diego, USA October 15-18, 2012:

- V.A. Izzo gave a presentation "Impurity Mixing and Radiation Asymmetry in MGI Simulations of DIII-D."

22ND International Toki Conference, in Toki, Japan November 19-22, 2012:

- O. Meneghini gave a presentation "On the OMFIT Modeling Framework and the Development of Steady State Scenarios for a Fusion Nuclear Science Facility."

2011 PRESENTATIONS

53RD APS DPP meeting in Salt Lake City, Utah November 14–18, 2011:

- N.W. Ferraro gave an invited presentation "Calculation of Linear Two-Fluid Plasma Response to Applied Non-Axisymmetric Fields."
- P.B. Snyder gave an invited presentation "The EPED Pedestal Model: Extensions, Experimental Tests, and Application to ELM-suppressed Regimes."

FSP Definition Workshop in San Diego, CA February 8-11, 2011:

- V.S. Chan gave a presentation "FSP Experimental Validation Overview."
- P.B. Snyder gave two presentations "The Pedestal Science Driver: Science Goals, Plan, and User Cases" and "Pedestal Validation: Examples of Current Practice and 3-5 Year Vision."

US-Japan RF Physics Workshop in Toba, Japan February 8-9 2011:

- M. Choi gave a presentation "Previous and Ongoing Benchmarking Activities on Self-Consistent ICRH Modeling."

ITPA Pedestal Topical Meeting in Cambridge, MA March 30 – April 1, 2011:

- N.W. Ferraro gave a presentation "Linear Stability and Response Calculations with Resistivity, Rotation, and Two-Fluid Effects."
- P.B. Snyder gave a presentation "Progress in the EPED Pedestal Model: Comparison to Hybrid and Baseline Discharges on JET."

Joint EU-US Transport Task Force Workshop in San Diego, CA April 6–9, 2011:

- P.B. Snyder gave a presentation "Developing and Testing the EPED Pedestal Model: Comparisons to Hybrid and Baseline Discharges on JET."

Stochasticity in Fusion Plasmas Workshop in Julich, Germany April 11–14, 2011:

- A.D. Turnbull gave an oral presentation "Plasma Response Models for Non-Axisymmetric Perturbations."

19TH Topical Conference on Radio Frequency Power in Plasmas in Newport, Rhode Island June 1–3, 2011:

- M. Choi gave a presentation "Modeling of Synergy between 4th and 6th Harmonic Absorptions of Fast Waves on Injected Beams in DIII-D Tokamak."

38TH European Physical Society Conference on Plasma Physics in Strasbourg, France June 27–July 1, 2011:

- G.M. Staebler gave an oral presentation "Multispecies Gyro-Kinetic Momentum Transport Modeling with the Trapped Gyro-Landau Fluid Model."

Integrated Technology Workshop at ITER Headquarters Cadarache, France June 8–10, 2011:

- L.L. Lao gave a presentation "Automated Reconstruction and Experimental Integrated Modeling and Data Analysis in DIII-D."

SciDAC 2011 Workshop in Denver, CO July 14, 2011:

- N.W. Ferraro gave an invited oral presentation "Fluid Modeling of Fusion Plasmas with M3D-C1."

ITPA MHD, Disruptions and Control Topical Meeting in Padova, Italy October 4-7, 2011:

- V.A Izzo gave a presentation "Recent Progress on NIMROD Simulations of Massive Particle Injection Including RE Orbits."

3. ADVANCES IN MHD EQUILIBRIUM AND STABILITY RESEARCH

3.1. 2D EQUILIBRIUM RECONSTRUCTION AND 3D LOCAL EQUILIBRIUM

EFIT Reconstruction with Ion-Temperature Constraints: The ECE electron temperature constraint in EFIT has been expanded to allow for the use of CER ion-temperature (T_i) data as additional measurements to constrain the internal flux-surface geometry across the measurement plane. T_i data can be input into EFIT in raw data form with measurements across a measurement plane or in processed-pairs form where the inboard and outboard temperatures are equal. Results from initial DIII-D EFIT reconstructions with CER T_i measurements as additional internal flux-surface constraints are promising and indicate that the constraints can be used to improve the inboard and outboard T_i overlapping.

Non-axisymmetric Local Toroidal Equilibrium: The initial formulation of 3D local equilibrium is completed. This is a true generalization of the Miller local equilibrium method for flux-surfaces that are good and nested, but not axisymmtric. A manuscript is underway. A new fully spectral approach to solving the neoclassical equations in 3D has also been outlined.

Non-Perturbative Non-axsiymmetric Effects in Local Equilibrium Solver: The new 3D local equilibrium solver LE3 has been upgraded to allow for larger (non-perturbative) non-axisymmetric components. The method is analogous to a 3D extension of the Miller local equilibrium method for shaped axisymmetric plasmas. Similar to Hegna's approach, LE3 is based on solving the MHD constraint equation representing the radial current equation. However, unlike previous approaches by Hegna, which specified a flux surface parameterization (R, Z) as a function of the straight field line angles and then used the $J_r = 0$ equation to solve for the Jacobian, we specify (R, Z) as a function of (r, θ_l, φ), where φ is the toroidal angle and θ_l is a new poloidal angle (equivalent to the Miller poloidal arc length in 2D), to solve for the mapping between θ_l and the straight field line angles to form the complete solution for the metric components of the magnetic coordinate mapping. Previous algorithms to solve this difficult 2D nonlinear PDE for θ_l using a fixed point iteration scheme was surprisingly fast but did not perform well for large non-axisymmetry, especially at large inverse aspect ratio. Attempts to improve on this with a Jacobian method (implicitness in all terms in θ_l and φ) were found to be unstable due to singularities in the derivative matrix. The new algorithm uses MINPACK to solve the equation with the full Jacobian is more robust, particularly with use of the 2D solution as an initial condition to enhance the

convergence. LE3 is being used to study the onset of stochasticity and will be coupled with NEO for 3D neoclassical transport studies of magnetic field ripple and resonant magnetic perturbations.

3.2. PEDESTAL AND ELM STUDIES

ELITE/EPED Pedestal and ELM Studies: The ELITE code has been used to study a broad database of discharges in which ELMs are suppressed with resonant magnetic perturbations (RMPs). It is consistently found that when ELMs are suppressed by RMPs, the discharges are stable to peeling-ballooning modes. In the absence of RMPs, the discharges approach the peeling-ballooning instability boundary and ELMs are observed.

The EPED model has been used in an initial study of pedestal structure in more than 300 JET discharges with the new ITER-like-wall (ILW). The initial study finds that EPED predicts the pedestal height in ILW discharges with similar (~20%) accuracy as earlier JET carbon-wall discharges. Much of the reported reduction in pedestal height with the ILW appears to be due to being able to achieve Type I ELMing at lower power, and therefore lower core beta (and hence the Shafranov shift, which improves edge stability, is lower), but significant effects due to lower impurity content are also indicated. A more detailed treatment of impurity effects is being incorporated into the EPED model to further develop this study.

The edge stability of an ELMing discharge in C-Mod has been investigated with ELITE as part of the 2013 Joint Research Target. The analysis is consistent with the ELM being triggered and the pedestal constrained by intermediate-wavelength peeling-ballooning modes.

Ballooning Criticality near Separatrix: A study of ballooning criticality near the separatrix in model equilibria based on DIII-D, JET, C-Mod and ITER has been conducted to explore possible connections to the observed Scrape-off-layer (SOL) width. Empirical scaling of SOL width observations suggests the possibility that the ITER SOL width may be very narrow, possibly 1mm or less, leading to concerns about divertor heat loads on ITER. An initial study of near-separatrix (ψ_N = 0.995) ballooning critical pressure scale lengths finds that observed SOL widths on existing devices (DIII-D, JET, C-Mod) are approximately consistent with ballooning criticality, but that ~1mm SOL widths for ITER would significantly exceed the ballooning critical width, suggesting that ballooning physics might lead to wider SOL widths on ITER. More detailed study is underway to pursue this possibility.

M3D-C1 and NIMROD Linear ELM benchmarking: The linear growth rates of peeling-ballooning modes were calculated using both M3D-C1 and NIMROD with models that include the full Braginskii gyroviscosity. The gyroviscosity is responsible for the "diamagnetic stabilization" that stabilizes moderate- to high-*n* peeling-ballooning modes. These calculations therefore include the diamagnetic stabilization effect fully self-consistently. The growth rates obtained using NIMROD and M3D-C1 were found to be in good agreement with each other. In the particular case studied, the self-consistent diamagnetic stabilization effect was found to be stronger than implied by the formula $\gamma^2 = \gamma^2_{ideal} - \omega^2_{*i}$, which is derived in the high-*n* limit (Fig. 1).

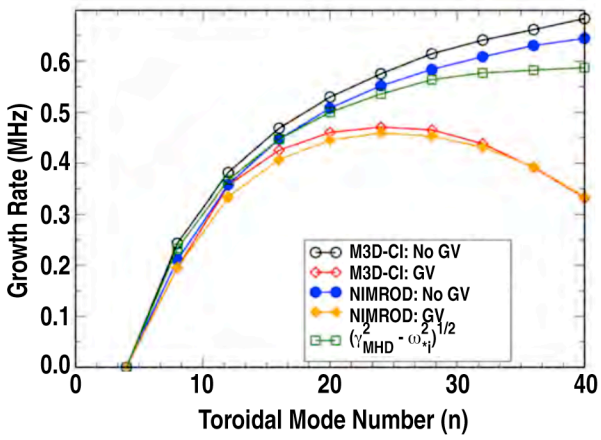

Fig. 1. Growth rate of the least-stable peeling ballooning mode as a function of toroidal mode number. Calculations that include gyroviscosity (GV) find a lower growth rate than those that do not (No GV) due to the diamagnetic stabilization effect. Growth rates from M3D-C1 and NIMROD are found to be in good agreement.

3.3. PLASMA RESPONSE TO EXTERNAL PERTURBATION FIELDS

Comparison of MARS, M3D-C1, and IPEC Linear Plasma Response: A more careful direct comparison of the linear responses between MARS-F, M3D-C1, and IPEC found remarkably good quantitative agreement in the amplitude of the response (Fig. 2). However, there is a puzzling relative phase shift on the inboard side when the phases on the outboard side are matched. The reasons are not understood, but it appears that the MARS-F calculations are finding a predominantly $m/n = 9/3$ mode at the 8/3 surface. There is a similar discrepancy found in the MARS-F results at the $q = 3$ surface. This remains to be investigated.

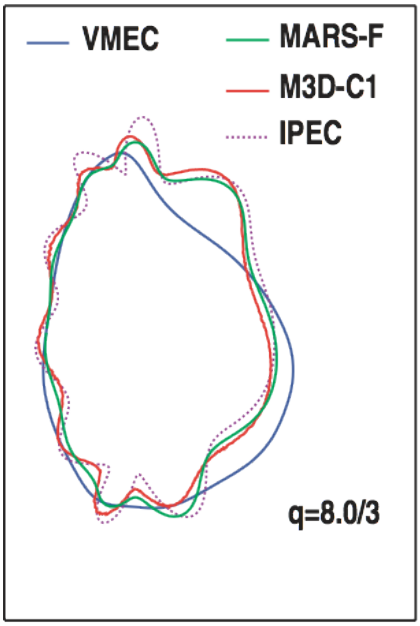

Fig. 2. The perturbed flux surface for DIII-D discharge #142603, as predicted by VMEC, MARS-F, M3D-C1, and IPEC. The perturbation is scaled up by factors of 56 for the MARS-F and M3D-C1 cases, a factor of 80 for IPEC, and a factor of 50 in VMEC.

M3D-C1 Edge Displacement Calculations: Calculations of the plasma response to applied 3D fields in the edge of DIII-D and ITER discharges have been carried out using M3D-C1 in support of the ITPA WG12 task led by I. Chapman. These calculations extended linear calculations that have recently been published by additionally considering the nonlinear response. It was found that the nonlinear calculations were generally in good agreement with the linear calculations for cases where the linear approximation was expected to remain valid. In addition, the M3D-C1 results were found to be in general agreement with JOREK calculations for the cases considered. The nonlinear M3D-C1 calculations were carried out using the Spitzer resistivity with realistic temperatures and diffusivities.

Effects of 3D Perturbations on Transport: A strong focus is now being placed on exploring the effects on transport of 3D perturbations, using perturbed equilibria calculated by M3D-C1 as a starting point for transport calculations. M3D-C1 simulation results indicate the potential for islands opening near the top of the H-mode pedestal in co-current rotating discharges, which suggests a mechanism for constraining the pedestal width in RMP ELM suppression. The expected transport due to stochastic fields at the top of the pedestal has not yet been quantified, but the transport due to the "magnetic flutter" in that region has been calculated for several DIII-D discharges.

Analysis of Non-Axisymmetric DIII-D Discharges with M3D-C1: The linear, two-fluid plasma response to applied non-axisymmetric fields has been calculated for a series of DIII-D discharges using M3D-C1, for various purposes. First, several discharges in various states of RMP ELM suppression were analyzed in order to determine the degree to which the edge response is dominated by kinking or island formation, and how strongly this result is affected by the proximity to ELM stability thresholds. It was found that the kink response is generally the dominant source of helical temperature and density perturbations in the pedestal region. This interpretation is consistent with SXR measurements, which show clear enhancement of SXR emission over predictions from vacuum modeling (which exclude kink response) in the pedestal.

Secondly, M3D-C1 calculations of DIII-D plasma response have been performed to provide a basis for transport calculations in non-axisymmetric equilibria. These transport calculations include magnetic flutter calculations, which find an enhancement of transport at the top of the pedestal (S. Smith). Other ongoing transport calculations using the fields calculated by M3D-C1 include ballooning mode stability calculations (T. Bird), and 3D gyro-kinetic calculations (D. Mikkelsen). The purpose of these calculations is to develop a predictive understanding of the effect of non-axisymmetric fields on pedestal structure, with the eventual goal of predictive models for RMP ELM suppression and density pump-out.

Finally, DIII-D discharges in which applied non-axisymmetric fields were found to affect the transport of beam ions have been modeled using M3D-C1. The non-axisymmetric densities, temperatures, and magnetic fields calculated by M3D-C1 have been used to study the effect on beam-ion birth profiles and transport by M. Van Zeeland. These calculations are proceeding with the goal of comparing the predicted transport with FILD fast-ion measurements. The ultimate goal of this work is to produce predictive models of the effect of non-axisymmetric fields on the confinement of fast ions (both beam ions and alphas).

M3D-C1 Response Calculations of DIII-D Experiments: Linear response calculations for 10 time slices of DIII-D discharge 148712 with alternating I-coil currents have been carried out. TRIP3D/MAFOT analysis of the M3D-C1 fields showed significantly increased stochasticity in the I-coil phase that leads preferentially to ELM suppression. The difference in response is attributed to differences in rotation. These differences are reduced as density increases. The linear response has also been calculated for limited L-mode plasmas exhibiting penetrated islands. Linear M3D-C1 calculations show the effect of applied torque on resonant field amplification, but do not show nonlinear bifurcation observed in experiment. Nonlinear calculations are planned.

Plasma response calculations of DIII-D ELM-suppression experiments with a reduced I-coil set using M3D-C1 have been carried out. These calculations include both the dominant $n = 3$ applied field, and the significant $n = 1, 2$, and 4 sidebands introduced by the reduced coil sets. In these cases, the sidebands contribute significantly to the predicted response and stochasticity.

A number of recent DIII-D experiments with applied RMP have been modeled using M3D-C1 to investigate differences between cases in which ELMs were successfully suppressed, and those in which they were not. In all cases, the plasma response has a qualitatively similar effect on the resonant components of the field, which are reduced in the pedestal (due to the diamagnetic electron flow), but amplified near the top of the pedestal.

The plasma response of several ELM-mitigated and ELM-suppressed discharges has also been calculated in order to estimate the electron thermal transport due to magnetic flutter. Calculations show strong enhancement of thermal transport near the top of the H-mode pedestal due to the penetration of islands there. (Although flutter transport does not depend on the presence of islands or stochasticity, the distortion of field lines is amplified by the presence of islands.)

3.4. GATO, MARS AND M3D-C1 DEVELOPMENTS AND IMPROVEMENTS

GATO Developments: The new script for stability runs for multiple eigenmodes was completed and appears to be working efficiently. For each eigenmode calculation, the initial eigenvalue guess is set from the history of the previous few eigenvalues so that a minimum number of iterations are required to converge to the desired one. The testing of the new kinetic energy norm in GATO using the new script to run through the stable modes behaves as expected.

MARS Improvements: Debugging of the new F90 FFT routines to replace the NAG library was completed and the new code is now ready for public release. In addition to a couple of inconsistencies that turned out to be insignificant, a serious bug was found and corrected for the case with partial walls. The new code will be placed in SVN but a stable public version will also be placed in a standard LINUX directory.

Resistive Wall Modeling in M3D-C1: Progress has been made in the development of a new resistive-wall model in M3D-C1. In this model, the resistive wall and vacuum region are included within the computational domain, which allows the treatment of resistive walls of arbitrary thickness. This capability will enable modeling of ITER, which is expected to be

in the "thick-wall" regime. Calculations including a resistive wall using the full, 7-field model in M3D-C1 have now been carried out successfully in 2D. Upcoming calculations will focus on modeling vertically unstable plasmas.

3.5. NIMROD DISRUPTION AND RUNAWAY ELECTRON MODELING

Massive Gas Injection (MGI) Simulations with Applied *n*=1 Fields: Two NIMROD simulations have been run in which a DIII-D discharge is terminated by Ne MGI while n=1 fields are applied in an attempt to influence the phase of the unstable 1/1 mode during the thermal quench (TQ). In MGI simulations without applied fields, the 1/1 mode always orients itself with a particular phase relative to the toroidal location of the gas jet source. In one simulation, the applied fields are aligned with the natural phase of the mode, while in the other, the applied fields have the opposing phase. In the latter simulation, the applied fields did not successfully force the unstable 1/1 mode to take on the opposite phase, but did delay the growth of the mode and reduce its amplitude. However, a larger radiated power spike was observed in that case. Simulations with larger amplitude applied fields are planned. These simulations suggest that measurable differences should be observed in the timing and amplitude of the measured radiated power in an upcoming DIII-D experiment, even if the mode is not successfully locked to the applied fields.

Comparison of NIMROD Predictions with DIII-D MGI Experiment: Simulations of massive gas injection with NIMROD produced several predictions about the importance of the n = 1 mode phase in determining the radiated power distribution and impurity mixing during the thermal quench (TQ). To test these predictions, a DIII-D experiment was carried out in July in which n = 1 fields were applied prior to each MGI shutdown in order to vary the phase of the n = 1 mode systematically. Analysis shows the TQ mode phase was successfully locked to the applied fields when the coils were activated 600 ms prior to the shutdown, but not with only a 50 ms delay. In those cases where the mode phase was locked, systematic variations versus phase in the temporal behavior and poloidal distribution of the radiated power were seen, with good reproducibility for a given phase. Density data also shows significant variation with phase, with more efficient impurity mixing seen for the phases at which this would be expected from the NIMROD predictions. Analysis and comparison of this data with simulations is ongoing, and further simulations will be carried out to model several of the discharges from this run day.

Runaway Loss Variation with Impurity Source Distribution during Rapid Shutdown Simulations with NIMROD: Runaway electron (RE) losses during DIII-D rapid shutdown simulations with NIMROD have been compared for a variety of injection scenarios. For the same equilibrium, edge localized "Massive Gas Injection-like" (MGI)

injection more thoroughly de-confines REs during the thermal quench than more uniform "pellet-like" injection. Toroidally uniform and toroidally localized MGI injection on the low-field-size show about the same RE behavior during the thermal quench (TQ), although the TQ happens earlier when the source is localized. For high-field-side injection, a significant fraction of the REs are de-confined just prior to (instead of during) the TQ, due to pre-TQ MHD modes that appear to produce RE losses without increasing radial heat transport enough to trigger a TQ. The reason for this difference will be studied in further simulations.

CQL3D / NIMROD Runaway Electron Study: In order to self-consistently investigate kinetic effects of runaway electrons under non-axisymmetric magnetic perturbations in tokamaks, the Fokker-Planck code CQL3D has been modified and interfaced with the 3D MHD code NIMROD. NIMROD computes radial profiles of plasma density, temperatures, electric field and magnetic perturbation as a function of flux surface coordinate. CQL3D reads these profiles and computes runaway-electron populations and their current density as a function of the flux surface coordinate. This information is passed back to NIMROD to further evolve the plasma density, temperatures, electric field and magnetic perturbation. In the previous version of CQL3D, the magnetic field perturbation could be applied only at one given flux surface. In the revised version, CQL3D reads the radial profile of the magnetic perturbation computed by NIMROD directly and computes the radial population of runaway electrons over the entire plasma radius.

Dependence of runaway electron confinement on MGI source: Runaway electron confinement in NIMROD simulations of massive gas injection in DIII-D has been compared for cases with toroidally peaked and toroidally symmetric gas sources, as well as for low field side (LFS) versus high-field side (HFS) injection. In the simulations, in which runaway electron losses were determined by test-particle orbits, toroidally localized sources were found to de-confine runaways earlier in time, consistent with an earlier growth of the $n = 1$ mode. For both HFS and LFS injection, increasing the toroidal peaking of the source produced slightly earlier runaway losses than a somewhat broader $n = 1$ gas distribution. Most notably, HFS injection was found to be especially effective at de-confining runaways. Unlike any other simulations, the two HFS injection cases showed significant losses of runaways prior to the growth and saturation of the $n = 1$ mode, indicating that the applied perturbation of the HFS gas jet itself can produce runaway losses across much of the plasma cross-section.

4. ADVANCES IN TRANSPORT RESEARCH

4.1. GYRO IMPROVEMENT AND NEW SOLUTION METHOD

GYRO OpenMP Improvement: The OpenMP implementation in GYRO has been re-engineered, with the effort led by an OpenMP expert (Bob Walkup) from IBM. The basic strategy has been to keep the number of parallel and work-sharing regions to a minimum, adding "!$omp barrier" where needed. Also, inner loops have been block partitioned. To accomplish this, the block-partitioned loop indices are computed once only and stored in a module. Some additional MPI-related improvements were accomplished by packing larger data objects into the repeated calls to MPI_ALLTOALL. On the IBM BlueGene/Q machine, the performance with 16 OMP threads is doubled in comparison to the original OpenMP implementation. What is particularly remarkable is that now, even for the small nl02a test case using 128 MPI tasks, we see cases with super-linear scaling: 2.5 times speedup on 2 OpenMP threads, and 4.3 times speedup with 4 OpenMP threads.

New 6D Fokker-Planck-Landau Equation Solution Method: A radically new method for solution of the Fokker-Planck-Landau equation is under development. This approach uses a Gaussian Radial Basis Function expansion, in terms of which exact matrix elements of the full 6D Fokker-Planck equation, with sources, can be obtained. Importantly, the matrix elements of the nonlinear Landau collision operator can be obtained exactly and in a form that is more compact than any other scheme that we are aware of (including the Pareschi or Greengard form). This approach may provide (1) a closure-free alternative to MHD, (2) a realistic method to calculate the solution of the kinetic equation in the vicinity of the separatrix, (3) a higher-accuracy alternative to gyrokinetic theory, (4) a new approach to compute non-thermal particle distributions (alphas, beams, etc.).

4.2. ENERGETIC PARTICLE STUDIES

GYRO Energetic-Particle Transport Development: GYRO has been updated to accommodate a kinetic species with an isotropic slowing-down distribution. This modification has been made to improve the accuracy of the Alfvén eigenmode (AE) stiff transport model for energetic particle (EP) profile prediction. The model assumes AE transport is stiff beyond the critical EP pressure gradient at which the instability appears. The slowing-down distribution is a more accurate representation of fusion alpha particles than the previously used Maxwellian distribution and is likely to yield a more accurate value for the threshold. Preliminary local and global stability calculations show a nominally lower growth

rate when the slowing-down distribution is used, with a correspondingly higher critical gradient.

4.3. DEVEOPMENT AND TESTING OF CYCLOKINETICS REDUCED MODEL

Reduced Model for 6D Cyclokinetics Testing the Breakdown of Gyrokinetics: Our current hyposthesis for explaining the more than 5-fold shortfall in near L-mode edge turbulence and transport in gyrokinetics simulations and transport models like TGLF (fitted to GYRO simulations) is that the nonlinear coupling to the (normally ignored) high frequency ion cyclotron modes at the high edge turbulence levels interrupts the gyro-averaging allowing higher transport levels. We reported in an invited talk at the APS-DPP 2012 meeting that GYRO simulations with ion drift-kinetics (and no gyro-averaging) substantially increase the low-k turbulence and transport intensity (3 to 4-fold). A reduced model for 6D cyclokinetics (CK) testing the breakdown of 5D gyrokinetics (GK) by following dynamics in the gyro-phase has been developed. To make a tractable first simulation test problem we will consider local homogeneous electrostatic ($E\times B$) turbulence in a straight shearless magnetic field decreasing in the radial direction, while suppressing ion motion and variation along the field. Electrons are nearly adiabatic and the ∇B drift and ion temperature gradients provide a simplified model of toroidal ITG mode turbulence.

The 4D CK is tested against 3D GK simulations in a new rCYCLO code being developed with a PKU grad student (Zhao Deng). The 4D-CK equations have been recently converted to gyro-phase Fourier harmonic form. If enough harmonic (say 8) are retained, the linear low-frequency 4D-CY dispersion matrix modes recover the 3D-GK modes (as well as the expected ion cyclotron modes). Time stepping the initial value linear equations recovers the leading linear modes with small enough time step.

Mr. Deng Zhao (a Peking University graduate student) recently coded for a more physical nonlinear collisional drift wave (CDW) electron model that is more appropriate to a very cold L-mode edge, where we hope to see a higher level of cyclokinetic transport than obtained from gyrokinetics. This may account for the missing L-mode edge transport. The rCYCLO code is actually three codes in one: a 3D gyrokinetic code (3D-GK), a 4D cyclokinetics code (4D-CK) written in cyclotron harmonics (3D-GK has only the "zeroth harmonic" low drift frequency harmonic), and a 4D gyro-phase angle Fourier harmonic (4D-FK) form of 4D-CK. 4D-CK is only used for linear check-outs since nonlinear 4D-CK seems numerically impractical: the formulation is just too complicated. The new CDW electron models (which also contains the resistive g-mode) linearly checked out perfectly across the three code sections. In the linear check out process, we discovered that all three 3D-GK, 4D-FK, and

4D-CK (with near adiabatic electrons and CDW electrons) has a spurious unstable high-k ITG mode. The problem was traced to the lack of curvature-drift drive resulting from the suppression of parallel motion (and variation) in going from 6D(5D) to 4D(3D). This was easily fixed by artificially doubling the ∇B drift and killing off the spurious high-k ITG modes. An important verification is that nonlinear 4D-FK transport must approach 3D-GK transport as the relative cyclotron frequency (inverse ρ^*) is made large enough (Just like General Relativity must approach Newtonian Gravity when gravity is weak enough.) We have yet to pass this test and we speculate that the spurious high-k ITG modes may have been the cause. When this test is passed the question becomes: does 4D-FK transport approach 3D-GK transport from above or below? Our hope is "from above". Mr. Zhao has now arrived at GA for a long-term visit and we expect progress to pick up.

4.4. TGLF TRANSPORT MODELING

TGLF Validation for High q_{min} DIII-D Discharges: While TGLF has been extensively validated for conventional sawtoothing H-modes and hybrids with $\beta_N < 2$, the model has not been validated for medium to high β_N discharges with elevated q_{min} values. As a result, its predictive capabilities for FDF AT scenarios have largely been unknown. To make progress in this area and to examine where the model may have issues accurately predicting the transport we have begun assembling a database of high q_{min} DIII-D discharges. To date, a database of 22 discharges has been constructed and the temperature profiles have been predicted using TGLF. We find that the RMS errors in the ion and electron temperatures for the 22 discharges are noticeably higher than what has been previously obtained for 40 DIII-D sawtoothing H-modes discharges. In particular, the RMS errors are 5% higher for Ti and 10% higher for Te.

TGLF Simulations of a DIII-D Double-Barrier QH-Mode Discharge: A well-diagnosed quiescent double barrier regime discharge that had a nearly stationary ITB was analyzed with XPTOR using TGLF plus NEO for neoclassical transport. All transport channels (electron particle, electron and ion energy, torodial rotation) were analyzed. The electrons, deuterium and carbon were all included as kinetic species for both TGLF and NEO with only the fast ions treated by the dilution approximation. The profiles were predicted from outside the ITB at $\varrho = 0.7$ into $\varrho = 0.1$. This discharge had very good agreement between the predicted and measured profiles for all channels (Fig. 3). If the same discharge was run with GLF23 plus NEO, it gives a run away electron density and toroidal rotation because the transport is reduced to neoclassical for these channels. This is a long-standing problem with GLF23 simulations since 1998. The fact that TGLF resolves the mystery of the

missing particle and momentum transport is a satisfying validation of gyro-kinetic theory and the progress that has been made since 1998 in gyro-kinetic simulation and quasi-linear modeling. Each transport channel is impacted in different ways by the various gyro-kinetic instability drives.

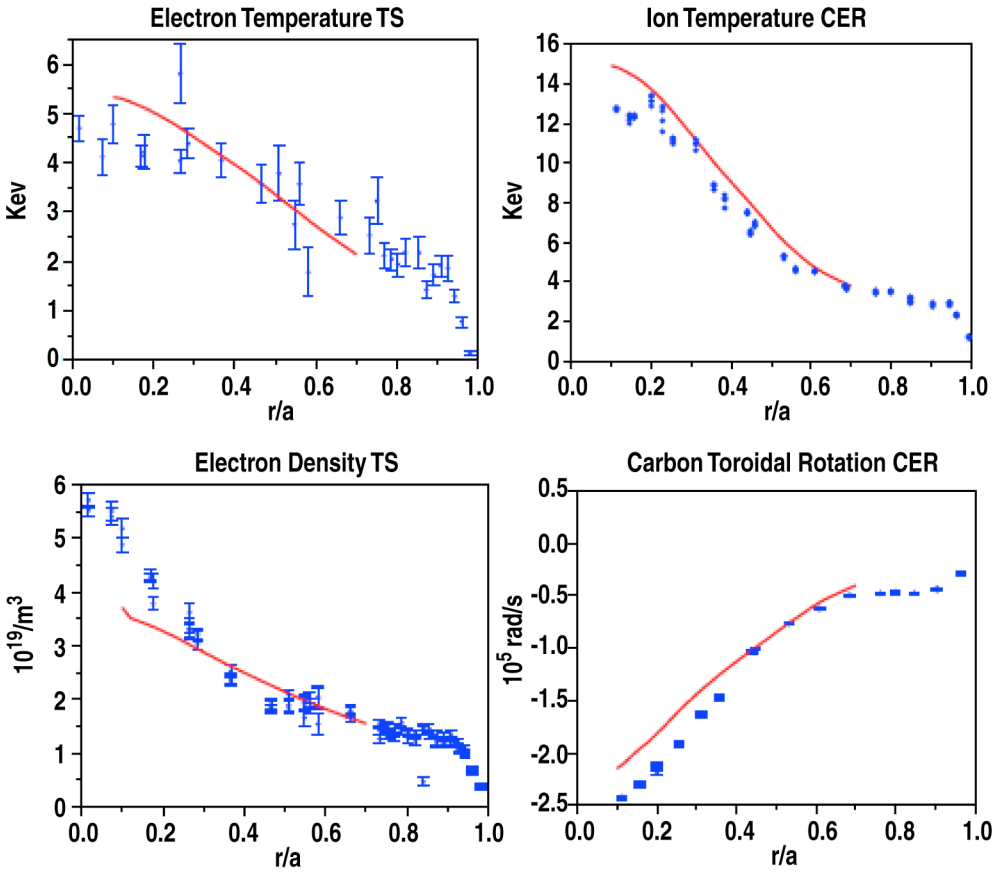

Fig. 3 Comparison of predicted profiles computed with TGLF, NEO, and the new spectral-shift paradigm for *E×B* shear suppression against experimental profiles for DIII-D QDB discharge 103740.

TGLF Simulations of DIII-D Discharges with Internal-Transport Barrier: A few more internal transport barrier cases were found and run with TGLF+NEO in XPTOR. Most have fairly substantial time derivatives. A fairly stationary weak ITB case with CER data on both sides of the magnetic axis was run to compare the predicted and measured poloidal flow. The ITB profiles (n_e, T_e, T_i, $V_{E\times B}$) were all predicted. The profile prediction is pretty good, but the measured polidal rotation does not agree with the NEO calculation in the ITB.

4.5. NEOCLASSICAL TRANSPORT AND BOOTSTRAP CURRENT

Asymptotic Theory of Neoclassical Transport in Rotating Plasmas: A scheme for the asymptoptic solution of the Braginski fluid equations for neoclassical transport in the Pfirsch-Schluter regime has been worked out. In particular, a simple method for working out the large-rotation limit was discovered. A manuscript is underway that will present valuable new NEO validation tests.

Bootstrap Current in the Plasma Edge: NEO has been used to study the accuracy of the Sauter model for the bootstrap current and the new formula by Koh et al, which is a modification of the former, designed to bring closer agreement between the XGC0 code and the Sauter model in the pedestal. For typical DIII-D plasmas, the Koh modification is negligible. However, for NSTX plasmas in the pedestal, the Koh formula predicts a much larger magnitude of the bootstrap current than the Sauter model. The NEO results generally follow the Sauter model, with a slightly lower value, and thus do not agree with the Koh modification formula. A simple example in s-α geometry illustrates that there is an anomaly in the Koh formula at large $\varepsilon = r/R$ related to the terms proportional to the temperature gradient. In this case, we set the ion neoclassical driving gradients to zero and retain only a moderate electron temperature gradient, which eliminates any caveats regarding steep gradients since the results scale linearly with ρ/L. At small ε, NEO, Sauter, and Koh agree reasonably well across a wide range of collisionality. But, as ε increases, the Koh formula develops a large spike near $\nu_e^* = 1$ which appears to be unphysical, in a region where NEO qualitatively agrees well with Sauter.

Analysis of Limitations of Bootstrap-Current Models Including Impurities: The drift-kinetic code NEO has been used to explore the accuracy and limitations of the Sauter model for bootstrap current. For a range of experimental DIII-D discharges, it is observed that the Sauter model over-estimates the bootstrap current at low collisionality, $\nu_e^* < 1$, with increasing error toward the banana regime, and largely underestimates the bootstrap current at high collisionality, with increasing error toward the Pfirsch-Schluter regime (Fig. 4).

For impure plasmas, the Sauter model is able to accurately capture the electron-impurity interaction through the use of Z_{eff} in ν_e^*, but does not accurately model the ion-impurity collisional interaction. However, the latter, that enters as a term proportional to the ion-temperature gradient, is often a sub-dominant contribution to the bootstrap current compared with the pressure gradient and electron-temperature gradient terms representing the former. Analysis of the Sauter model for energetic impurities shows that it largely over-estimates the collisional effect of the energetic species on the ion and electron dynamics. This may have

implications for the modeling of reactors like ITER that are expected to have a significant concentration of alpha particles.

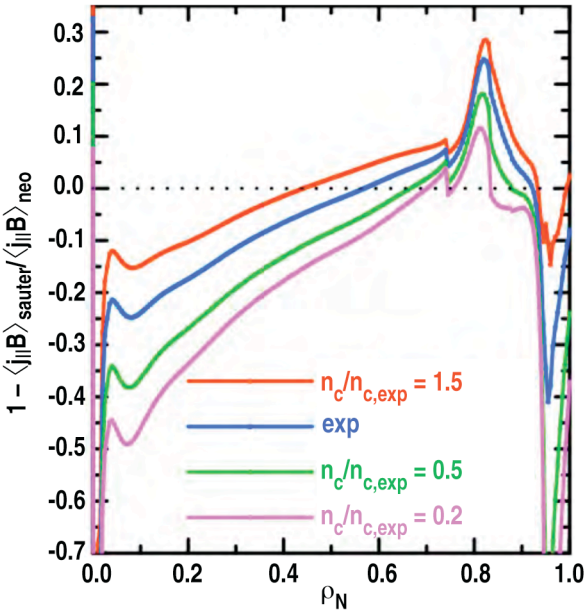

Fig. 4. Fractional bootstrap current difference computed using the Sauter bootstrap current model and NEO for DIII-D discharge 145934 with various concentrations of carbon impurity.

4.6. TRANSPORT DUE TO RMP FIELDS

Quasi-linear Transport from External Magnetic-Field Perturbations: The new RMPtran code calculates the quasi-linear transport from external Resonant Magnetic Perturbation (RMP). RMPtran takes the linear collisional-Braginskii two-fluid responses from the M3D-C1 code to calculate the instantaneous quasi-linear particle and toroidal angular momentum (TAM) transport. These flows as well the energy transport flows are proportional to the square of the screened external magnetic perturbations δB^2. The focus of RMPtran is on understanding the DIII-D RMP density pump out effect: when the RMP coils are switched on, why does most of the TAM leave the plasma by particle convection rather than slowing the toroidal rotation as expected?

First results indicate a huge RMP induced $E\times B$ particle transport at the edge that may explain the density pump. TAM transport is broken into the Reynolds stress on the plasma and Maxwell stress on the plasma and field that results from the RMP applied $J\times B$ torque density. Most of the $J\times B$ torque is from the displacement radial current leaving little Maxwell stress on the plasma. (The distinction between Maxwell stress on the plasma field

and Maxwell stress on the plasma alone seems to have been ignored in all previously published work, including our own published work. The reason seems to be because the TAM contained in the field is well known to be so much less than that contained in the plasma.) Over the inner core ($r/a < 0.8$) much of this Maxwell stress on the plasma appears to be cancelled by the Reynolds stress. To understand the pump-out effect, we must compare and contrast the core and edge instantaneous flows just after RMP turn-on to those well after turn-on.

5. ADVANCES IN INTEGRATED MODELING, RF HEATING, AND FUELING RESEARCH

5.1. OMFIT DEVELOPMENT AND APPLICATIONS

OMFIT Development: OMFIT (One Modeling Framework for Integrated Tasks) is a new software package developed to support integrated modeling and experimental planning. The main idea at the base of OMFIT is to treat files, data and scripts as a uniform collection of objects organized into a tree structure. The OMFIT framework provides a consistent way to access and manipulate such collection of heterogeneous objects, independent of their origin. Within the OMFIT tree, data can be copied or referred from one node to another and tasks can call each other allowing for complex compound task to be built. Such uniform structure allows the definition of a single top-level Graphical User Interface (GUI), to manage tree objects, carry out simulations and analyze the data interactively. OMFIT has the ability to understand many scientific data format. When a file is loaded into OMFIT, its data populates the OMFIT tree, automatically endowing it with many potential uses. Furthermore, integration with MDS+ tree allows direct manipulation of the experimental data.

In OMFIT modeling tasks are organized into modules, which can be easily combined to create arbitrarily large multi-physics simulations. Modules inter-dependencies are defined by referencing variables among them. The current version of OMFIT includes modules for magnetic, MSE and kinetic constrained equilibrium reconstruction (EFIT), transport (ONETWO), stability (PEST3) and ray-tracing (GENRAY) analysis. Creation of new modules and customization of existing ones is encouraged and simplified by the availability of high level Python Application Programmer Interfaces (APIs) for the execution of codes on remote servers and creation of application specific GUIs. The NEO drift-kinetic neoclassical transport module is also available under OMFIT to provide an accurate evaluation of neoclassical transport fluxes and bootstrap current for use with other physics modules (Fig. 5). Visualization of experimental and modeling data is possible within OMFIT, for both quick analysis and publication.

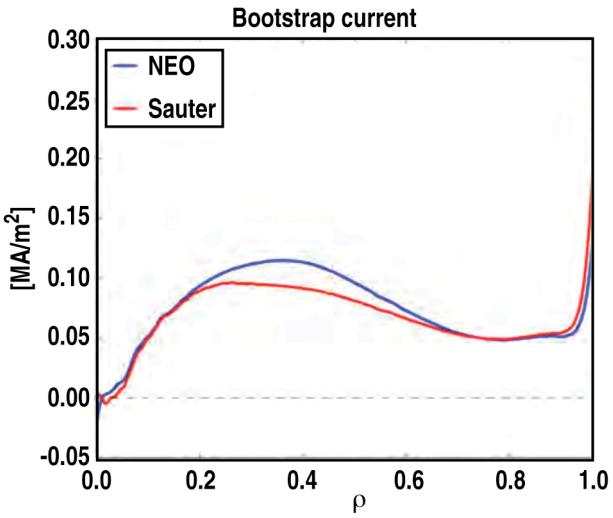

Fig. 5. Bootstrap current computed using NEO under OMFIT for DIII-D discharge 145701. Also shown is the bootstrap current computed using the Sauter bootstrap current model.

OMFIT Edge Stability Application: The OMFIT integrated modeling framework has been extended to enable analysis of DIII-D kinetic profiles in presence of ELMs. This was achieved by binning and organizing the experimental data as a function of the ELM cycle. A GUI guides users throughout this process. The resulting electron density and temperature profiles can be used in any of the OMFIT modules. For example, ELM-aware kinetic EFITs have been used to assess the edge stability of DIII-D discharges. The experimental pressure and current profiles at the edge of the experimentally reconstructed equilibrium is perturbed via the new VARYPED module in OMFIT. The stability of the resulting set of equilibria is then tested with the ELITE code (also a new OMFIT module). Results compare well with previous findings and show that the steep experimental profiles occurring before an ELM crash are indeed at the boundary of the stability limit (Fig. 6).

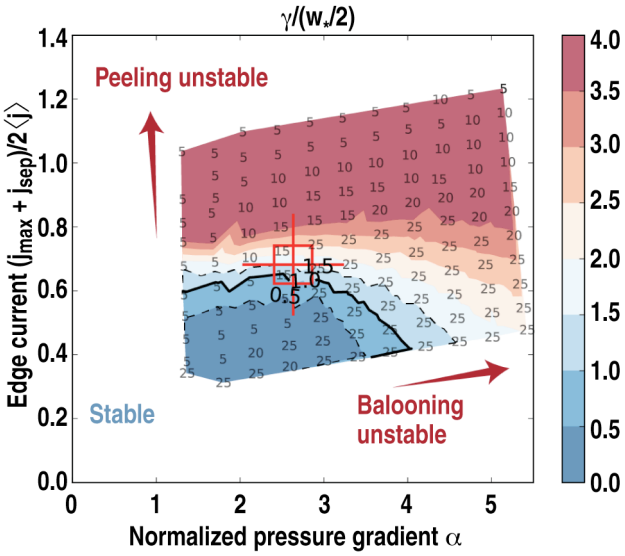

Fig. 6. Edge peeling-ballooning stability diagram computed with ELITE under OMFIT for DIII-D ELMing H-mode discharge 131997.

5.2. ONETWO TRANSPORT CODE DEVELOPMENT

ONETWO Development: A new ONETWO version 5.49 has been released and is now being adopted by the Auto-ONETWO group as the new standard version. Various refinements were introduced to speed up both the RF calls and the P-NFREYA execution time. The state file was significantly expanded to accommodate new physics output, including the introduction of aneutronic He^3 fusion. The enhanced spin polarized cross section for this fusion reaction is currently modeled by an isotropic Bosch-Hale cross section averaged over all possible spin states. Anisotropic, spin dependent reaction rates may be included in the future, pending evaluation of the current results. Deuterium beams interacting with thermal He^3 is of primary experimental interest, so some effort was expended in determination of beam-thermal reaction rates. Regression testing, which is still underway, has not revealed any issues.

GCNMP, the parallel version of ONETWO, was modified to allow specification of generalized boundary conditions. This required a significant restructuring of the finite difference form of the particle and energy transport equations. By allowing a linear combination of flux and profile gradient values to be specified at the boundary, it is possible to generate new solutions that may have application in the transition to the boundary layer at the plasma edge. We note that such boundary conditions do not guarantee the existence of steady-state solutions. However, the method seems to be particularly suitable for modeling DIII-D discharges since the power balance flux at the plasma edge can be used to define the

mixed (Robin) boundary conditions. This is expected to shed new light on turbulent transport modeling of DIII-D discharges. Using the method for analysis of advanced tokamaks such as FNSF has shown that there is a small window of possible boundary conditions that will yield acceptable AT-type steady-state conditions. Current modeling of FNSF with hollow current profiles has shown that it is possible to generate non-inductive steady-state scenarios, but MHD equilibrium is problematic due to the formation of very elongated plasma contours near the magnetic axis. Robin-type boundary conditions applied to this scenario can be used to eliminate the discontinuity of the energy flux typically observed if the boundary is taken at values of $\rho < 1$.

As part of the restructuring of the finite difference form of the transport equations, some numerical experimentation using an idea originally put forward by Perverzev-Corrigan was implemented. This method relies on using different fluxes in the predictor and corrector steps of the numerical scheme. Thus, the time evolvement of the solution may not be followed exactly, but a more rapid approach to a steady state is possible. Applied to FNSF it was shown that a speedup of 15 was achieved with essentially the same final steady state result.

5.3. ORBIT-RF SIMULATIONS

ORBIT-RF Simulations of DIII-D High-Harmonic Fast-Wave Experiments: For quantitative comparison of computed fast-ion distributions with measurements, a series of self-consistent simulations using the 5D finite-orbit Monte-Carlo code ORBIT-RF coupled with the full-wave code AORSA was performed by scanning the assumed fraction of core fast-wave (FW) power absorption. The fast-ion distributions that yield the neutron enhancement factor comparable to the experimental ones are passed to the fast-ion diagnostic simulation code FIDASIM to compute the synthetic fast-ion D_α (FIDA) signals. ORBIT-RF/AORSA reproduces the synergistic effect measured in neutron reaction rates and vertical FIDA signals in the two-frequency FW heating (4th harmonic 60 MHz and 6th harmonic 90 MHz) compared to those obtained in a single-frequency FW heating (4th harmonic 60 MHz). For the tangential FIDA signals, ORBIT-RF/AOSA also reproduces the trend of the measured FIDA signals, which indicate that the tangential components of the fast ions are hardly accelerated by either a single-frequency FW or two-frequency FW. This synergy arises from finite Larmor radius effects that occur since a substantial fraction of fast ions above the neutral-beam injection energy is present due to preheating by the 60 MHz FW. Therefore, the additional 90 MHz FW damps significantly on the beam-ion tails and produces a synergy.

5.4. PELLET FUELING STUDIES

Pellet Ablation Modeling: Work continued on the pellet ablation modeling under a unified theoretical framework covering both $Z > 1$ icy pellets and refractory pellets, where Z is the atomic number of the pellet specie. We considered a new composite pellet: a beryllium pellet core with a thin outer shell of Li for ITER and for DIII-D a boron shell with a thin outer layer of Li or a porous boron pellet coated with Li. The shell aspect ratio and the porosity of boron were varied so as to keep the same boron mass deposited in the DIII-D plasma from r/a = 0.65 to r/a = 0. For a number of different pellet configurations we then calculated the pellet velocity needed to penetrate all the way to the magnetic axis r/a = 0. Given that velocity, we then calculated the Li layer thickness needed to get the Li layer to burn off exactly at r/a = 0.65 and expose the boron.

The purpose of the Li layer is to prevent a "normal" thermal quench (TQ), i.e., a TQ triggered by excessive cooling near the q = 2 surface. The Li deposition avoids excessive cooling because Li is a very weak radiator and pure Li pellets are known from prior experience on TFTR and C-Mod not to cause disruptions. Since the ablated Li will not cool the edge too rapidly, we can avoid the usual sequence of events: (1) current contraction near q = 2, (2) low-frequency MHD instabilities (3) magnetic ergodicity, and finally (4) fast core heat transport. Therefore the pellet will ablate in the hot undisturbed plasma without hitting the far wall, as would be the case when a cooling wave races ahead of the pellet, for example, as in the case of an argon pellet injection in DIII-D. The purpose of using the porous/shell boron pellet is to shorten the pellet ablation time for a given mass, thus requiring a faster velocity needed to penetrate to the core, to ensure that the pellet velocity exceeds the velocity of the cooling wave.

Shatter Pellet Fracture Study: Spallation or disintegration of a large solid deuterium pellet into daughter fragments upon impact with a rigid surface is under investigation as a method of producing a collimated stream of small pellets for disruption mitigation in ITER. We propose that the fracture of the pellet is caused by tensile loading brought about during the initial impact and generation of stress waves that interact upon reflection from the free surface of the "brittle" pellet. The concept of (reversible) surface free energy was used to calculate the total surface area increase due to the many fragments produced after the impact. This together with the conservation of momentum, energy and volume before and after impact allows us to estimate the (average) size and number of daughter fragments produced as a function of initial pellet size, impact velocity, and trajectory obliquity. Strain energy

dissipation, an extra irreversible energy cost process, was neglected in this analysis but will be included in future work.

Oak Ridge National Laboratory (ORNL) is investigating the technology for shattering a large, high-speed cryogenic pellet into many smaller fragments before it enters a hot pre-disruption plasma. The debris cloud formed by the dispersal of the small fragments will be more easily ablated and assimilated in the plasma than a large intact pellet, which would pass unablated through the plasma discharge, striking the far wall of the ITER. Under high-velocity impact with a solid target, the pellet material is subjected to large impact stresses, causing the pellet to fracture into a cloud of smaller fragments. The tensile stress is the primary agent for shattering the pellet because pre-existing flaws and cracks will propagate under tensile load. Improving the understanding of the timescales and conditions under which these processes occur is of great value to the success of the shatter pellet approach for disruption mitigation in ITER.

6. PUBLICATIONS

GA THEORY PUBLICATIONS FOR 2013

M. Barnes, F.I. Parra, J.P. Lee, E.A. Belli, M.F.F. Nave, and A.E. White, "Intrinsic Rotation Driven by Non-Maxwellian Equilibria in Tokamak Plasmas," Phys. Rev. Lett. **111**, 055005 (2013).

E.M Bass and R.E. Waltz, "Gyro-Kinetic Study of the unstable Alfven Eigenmode Spectrum in a Reversed Shear Discharge," Phys. Plasmas **20**, 012508 (2013).

L. R. Baylor, N. Commaux, T. C. Jernigan, N. H. Brooks, S. K. Combs, T. E. Evans, M. E. Fenstermacher, R. C. Isler, C. J. Lasnier, S. J. Meitner, R. A. Moyer, T. H. Osborne, P. B. Parks, P. B. Snyder, E. J. Strait, E. A. Unterberg, and A. Loarte, "Reduction of ELM Intensity Using High-Repetition-Rate Pellet Injection in Tokamak H-Mode Plasmas," Phys. Rev. Lett. **110**, 245001 (2013).

M.N.A. Beurskens, L. Frassineeti, C. Challis, T. Osborne, P.B. Snyder, et al., "Comparison of Hybrid and Baseline ELMy H-Mode Confinement in JET with the Carbon Wall," Nucl. Fusion **53**, 013001 (2013).

D.P. Boyle, J.M. Canik, R. Maingi, P.B. Snyder, and T.H. Osborne, "Varying the Pre-Discharge Lithium Wall Coatings to Alter the Characteristics of ELM-free H-Mode Pedestal in NSTX," Nucl. Fusion **53**, 013001 (2013).

K.H. Burrell, A.M. Garofalo, W.M. Solomon, M.E. Fenstermacher, D.M. Orlov, T.H. Osborne, J.-K. Park and P.B. Snyder, "Quiescent H-Mode Operation Using Torque from Non-Axisymmetric, Non-Resonant Magnetic Fields," Nucl. Fusion **53**, 073038 (2013).

J. Candy, "Turbulent Energy Exchange: Calculation and Relevance for Profile Prediction," Phys. Plasmas **20**, 082503 (2013).

N.M. Ferraro, T.E. Evans, L.L. Lao, R.A. Moyer, R. Nazikian, D.M. Orlov, M.W. Shafer, E.A. Unterberg, M.R. Wade, and A. Wingen, "Role of Plasma Response in Non-Axisymmetric Tokamak Edge Displacements," Nucl. Fusion **53**, 073042 (2013).

B.A. Grierson, K.H. Burrell, W.M. Solomon, R.V. Budny and J. Candy, "Collisionality Scaling of Main-Ion Toroidal and Poloidal Rotation in Low Torque DIII-D Plasmas," Nucl. Fusion **53**, 063010 (2013).

W. Guttenfelder, J. L. Peterson, J. Candy, S. Kaye, Y. Ren, R. E. Bell, G. Hammett, B. P. LeBlanc, D. Mikkelsen, W. M. Nevins and H. Yuh, "Progress in Simulating Turbulent Electron Thermal Transport in NSTX, " Nucl. Fusion **53**, 093022 (2013).

J.D. Hanson, D.T. Anderson, M. Cianciosa, P. Franz, J.H. Harris, G.H. Hartwell, S.P. Hirshman, S.F. Knowlton, L.L. Lao, E.A. Lazarus, L. Marrelli, D.A. Maurer, J.C. Schmitt, A.C. Sontag, B.A. Stevenson, and D. Terranova, "Non-Axisymmetric Equilibrium Reconstruction for Stellarators, Reversed Field Pinches and Tokamaks," Nucl. Fusion **53**, 083016 (2013)..

C. Holland, J.E. Kinsey, J.C. DeBoo, K.H. Burrell, T.C. Luce, S.P. Smith, C.C. Petty, A.E. White, T.L. Rhodes, L. Schmitz, E.J. Doyle, J.C. Hillesheim, G.R. McKee, Z. Yan, G. Wang, L. Zeng, B.A. Grierson, A. Marinoni, P. Mantica, P.B. Snyder, R.E. Waltz, G.M. Staebler and J. Candy, "Validation Studies of Gyrofluid and Gyrokinetic Predictions of Transport and turbulence stiffness using the DIII-D tokamak,"Nucl. Fusion **53**, 083027 (2013).

N.T. Howard, A.E. White, M. Greenwald, M.L. Reinke, J. Walk, C. Holland, J. Candy, and T. Görler, "Investigation of the Transport Shortfall in Alcator C-Mod L-Mode Plasmas," Phys. Plasmas **20**, 032510 (2013).

J.W. Hughes, P.B. Snyder, J.R. Walk, et al., "Pedestal Structure and Stability in H-Mode and I-Mode: A Comparative Study in Alcator C-Mod," Nucl. Fusion **53**, 043016 (2013).

V.A. Izzo, "Impurity Mixing and Radiation Asymmetry in Massive Gas Injection Simulations of DIII-D," Phys Plasmas **20**, 056107 (2013).

G.L. Jackson, V.S. Chan, and R.D. Stambaugh, "An Analytic Expression for the Tritium Burnup Fraction in Burning-Plasma Devices," Fusion Sci. Technol. **64**, 8 (2013).

H. Kim, L. Zhang, R. Samulyak, and P. Parks, "On the Structure of Plasma Liners for Plasma Jet Induced Magnetoinertial Fusion," Phys. Plasmas 20, 022704 (2013).

M.J. Lanctot, R.J. Buttery, J.S. de Grassie, T.E. Evans, N.M. Ferraro, J.M. Hanson, S.R. Haskey, R.A. Moyer, R. Nazikian, T.H. Osborne, D.M. Orlov, P.B. Snyder, M.R. Wade and the DIII-D Team, "Sustained suppression of type-I edge-localized modes with dominantly n = 2 magnetic fields in DIII-D," Nucl. Fusion **53**, 083019 (2013).

G.Q. Li, Q.L. Ren, J.P. Qian, L.L. Lao, S.Y. Ding, Y.J. Chen, Z.X. Liu, B. Lu, and Q. Zang, "Kinetic Equilibrium Reconstruction on EAST Tokamak," to appear in Plasma. Phys. Control. Fusion, 2013.

O. Meneghini and L.L. Lao, "Integrated Modeling of Tokamak Experiments with OMFIT," Plasma Fusion Res. **8**, 2403009 (2013).

P. Parks and W. Wu, "Modeling Penetration and Plasma Response of a Dense Neutral Gas Jet in a Post Thermal Quenched Plasma," submitted to Nucl. Fusion.

I. Pusztai, A. Mollén, T. Fülöp and J. Candy, "Turbulent Transport of Impurities and Their Effect on Energy Confinement," Plasma Phys. Control. Fusion **55**, 074012 (2013).

G.M. Staebler, J.E. Kinsey, and R.E. Waltz, "A New Paradigm for Suppression of Gyro-Kinetic Turbulence by Velocity Shear," Phys. Rev. Lett. 110, 055003 (2013).

G.M. Staebler, J. Candy, R.E. Waltz, J.E. Kinsey and W.M. Solomon, "A New Paradigm for $E \times B$ Velocity Shear Suppression of Gyro-Kinetic Turbulence and the Momentum pinch," Nucl. Fusion **53**, 113017 (2013).

M.S. Tillack, A.D. Turnbull, C.E. Kessel, N. Asakura, A.M. Garofalo, C. Holland, F. Koch, Ch. Linsmeier, S. Lisgo, R. Maingi, R. Majeski, J. Menard, F. Najmabadi, R. Nygren, T.D. Rognlien, D.D. Ryutov, R.D. Stambaugh, P.C. Stangeby and D.P. Stotler, "Summary of the ARIES Town Meeting: "Edge Plasma Physics and Plasma Material Interactions in the Fusion Power Plant Regime," Nucl. Fusion 53, 027003 (2013).

B. Tobias, L. Yu, C.W. Domier, N.C. Luhmann, Jr., M.E. Austin, C. Paz-Soldan, A.D. Turnbull and the DIII-D team, "Boundary Perturbations Coupled to Core 3/2 Tearing Modes on the DIII-D Tokamak," Plasma Phys. Control. Fusion **55**, 095006 (2013).

A.D. Turnbull, N.M. Ferraro, V.A. Izzo, E.A. Lazarus, J-K. Park, Q.A. Cooper, S.P. Hirshman, L.L. Lao, M.J. Lanctot, S. Lazerson, Y.Q. Liu, A. Reiman, and F. Turco, "Comparisons of Linear and Nonlinear Plasma Response Models for Non-Axisymmetric Perturbations," Phys. Plasmas **20**, 056114 (2013).

R.E. Waltz and Z. Deng, "Nonlinear Theory of Drift-Cyclotron Kinetics and the Breakdown of Gyro-kinetics," Phys. Plasmas **20**, 012507 (2013).

R.E. Waltz, E.M. Bass, and G.M. Staebler, "Quasilinear Model for Energetic Particle Diffusion in Radial and Velocity Space," Phys. Plasmas **20**, 042510 (2013).

A.E. White, N.T. Howard, M. Greenwald, M.L. Reinke, C. Sung, S. Baek, M. Barnes, J. Candy, A. Dominguez, D. Ernst, C. Gao, A.E. Hubbard, J.W. Hughes, Y. Lin, D. Mikkelsen, F. Parra, M. Porkolab, J.E. Rice, J. Walk, S.J. Wukitch, and Alcator C-Mod Team, "Multi-Channel Transport Experiments at Alcator C-Mod and Comparison with Gyrokinetic Simulations," Phys. Plasmas **20**, 056106 (2013).

S.K. Wong and V.S. Chan, "Electron Perpendicular Viscosity in Braginskii's Equations," Phys. Plasmas **20**, 074502 (2013).

X.Q. Xu, P.W. Xi, I. Joseph, M. V. Umansky, T. Y. Xia, B. Gui, S. S. Kim, G. Y. Park, T. Rhee, H. Jhang, P. H. Diamond, B. Dudson, and P. B. Snyder "Gyro-fluid and Two-fluid Theory and Simulations of Edge Localized Modes," Phys. Plasmas 20 056113 (2013).

GA THEORY PUBLICATIONS FOR 2012

E. Belli and J. Candy, "Full Linearized Fokker-Planck Collisions in Neoclassical Transport Simulations," Plasmas Phys. Control. Fusion 54, 015015 (2012).

K.H. Burrell, A.M Garofalo, W.M. Solomon, M.E. Fenstermacher, T.H. Osborne, J.-K. Park, M.J. Schaffer, and P.B. Snyder, "Reactor-Relevant Quiescent H-Mode Operation Using Torque from Non-Axisymmetric, Non-Resonant Magnetic Fields," Phys. Plasmas 19, 056117 (2012).

R. J. Buttery, A. H. Boozer, Y. Q. Liu, J.-K. Park, N. M. Ferraro, V. Amoskov, Y. Gribov, R. J. La Haye, E. Lamzin, J. E. Menard, M. J. Schaffer, E. J. Strait, and DIII-D Team, "The Limits and Challenges of Error Field Correction for ITER," Phys. Plasmas 19, 056111 (2012).

N.M. Ferraro, "Symmetries of Resistive Two-Fluid Magnetohydrodynamics under Reversal of Toroidal Field, Current, and Rotation," Phys. Plasmas **19**, 014505 (2012).

N.M. Ferraro, "Calculations of Two-Fluid Linear Response to Non-Axisymmetric Fields in Tokamaks," Phys. Plasmas **19**, 056105 (2012).

W. Guttenfelder, J. Candy, S. M. Kaye, W. M. Nevins, E. Wang, J. Zhang, R. E. Bell, N. A. Crocker, G. W. Hammett, B. P. LeBlanc, D. R. Mikkelsen, Y. Ren, and H. Yuh, "Simulation of Micro-Tearing Turbulence in National Spherical Torus Experiment," Phys. Plasmas 19, 056119 (2012).

W. Guttenfelder, J. Candy, S.M. Kaye, W.M. Nevins, R.E. Bell, G.W. Hammett, B.P. LeBlanc and H. Yuh, "Scaling of Linear Micro-Tearing Stability for a High Collisionality National Spherical Torus Experiment Discharge," Phys. Plasmas **19**, 022506 (2012).

C. Holland, J.C. DeBoo, T.L. Rhodes, L. Schmitz, J.C. Hillesheim, G. Wang, A.E. White, M.E. Austin, E.J. Doyle, W.A. Peebles, C.C. Petty, L. Zeng and J. Candy, "Testing Gyrokinetic Simulations of Electron Turbulence," Nucl. Fusion **52**, 063028 (2012).

C. Holland, C.C. Petty, L. Schmitz, K.H. Burrell, G.R. McKee, T.L. Rhodes and J. Candy, "Progress in GYRO Validation Studies of DIII-D H-Mode Plasmas," Nucl. Fusion **52**, 114007 (2012).

E.M. Hollmann, D.A. Humphreys and P.B. Parks, "Simulation of Main Chamber Wall Temperature Rise Resulting from Massive Neon Gas Injection Shutdown of ITER," Nucl. Fusion 52, 033001 (2012).

N.T. Howard, M. Greenwald, D.R. Mikkelsen, M.L. Reinke, A.E. White, D. Ernst, Y. Podpaly, and J. Candy, "Quantitative Comparison of Experimental Impurity Transport with Nonlinear Gyrokinetic Simulation in an Alcator C-Mod L-mode Plasma," Nucl. Fusion **52**, 063002 (2012).

N.T. Howard, M. Greenwald, D.R. Mikkelsen, A.E. White, M.I. Reinke, D. Ernst, Y. Podpaly and J. Candy, "Measurement of Plasma Current Dependent Changes in Impurity Transport and Comparison with Nonlinear Gyro-Kinetic Simulation," Phys. Plasmas **19**, 056110 (2012).

V.A. Izzo, D.A. Humphrey, and M. Kornbluth, "Analysis of Shot-to-Shot Variability in Post-Disruption Runaway Electron Currents for Diverted DIII-D Discharges," Plasmas Phys. Control. Fusion **54**, 095002 (2012).

A.N. James, M.E. Austin, N. Commaux, N.W. Eidietis, T.E. Evans, E.M. Hollmann, D.A. Humphreys, A.W. Hyatt, V.A. Izzo, T.C. Jernigan, R.J. La Haye, P.B. Parks, E.J. Strait, G.R. Tynan, J.C. Wesley and J.H. Yu, "Measurements of Hard X-Ray Emission from Runaway Electrons in DIII-D," Nucl. Fusion 52, 013007 (2012).

S.C. Jardin, N. Ferraro, J. Breslau and J. Chen, "Multiple Timescale Calculations of Sawteeth and Other Global Macroscopic Dynamics of Tokamak Plasmas," Comput. Sci. Disc. 5, 014002 (2012).

H. Kim, R. Samulyak, L. Zhang, and P. Parks, "Influence of Atomic Processes on the Implosion of Plasma Liners," Phys. Plasmas 19, 082711 (2012).

R. Maingi, D.P. Boyle, J.M. Canik, S.M. Kaye, C.H. Skinner, J.P. Allain, M.G. Bell, R.E. Bell, S.P. Gerhardt, T.K. Gray, M.A. Jaworski, R. Kaita, H.W. Kugel, B.P. LeBlanc, J. Manickam, D.K. Mansfield, J.E. Menard, T.H. Osborne, R. Raman, A.L. Roquemore, S.A. Sabbagh, P.B. Snyder and V.A. Soukhanovskii, "The Effect of Progressively Increasing Lithium Coatings on Plasma Discharge Characteristics, Transport, Edge Profiles and ELM Stability in the National Spherical Torus Experiment," Nucl. Fusion 52, 083001 (2012).

S. Mordijck, E. J. Doyle, G. R. McKee, R. A. Moyer, T. L. Rhodes, L. Zeng, N. Commaux, M. E. Fenstermacher, K. W. Gentle, H. Reimerdes, O. Schmitz, W. M. Solomon, G. M. Staebler, and G. Wang, "Changes in Particle Transport as a Result of Resonant Magnetic Perturbations in DIII-D," Phys. Plasmas 19, 079903 (2012).

R.A. Moyer, M.A. Van Zeeland, D.M. Orlov, A.Wingen, T.E. Evans, N.M. Ferraro, J.M. Hanson, R. Nazikian, M.R. Wade, and L. Zeng, "Measurement of Plasma Boundary Displacement by n=2 Magnetic Perturbations Using Imaging Beam Emission Spectroscopy," Nucl. Fusion 52, 123019 (2012).

J. L. Peterson, R. Bell, J. Candy, W. Guttenfelder, G. W. Hammett, S. M. Kaye, B. LeBlanc, D. R. Mikkelsen, D. R. Smith, and H. Y. Yuh, "Suppressing Electron Turbulence and Triggering Internal Transport Barriers with Reversed Magnetic Shear in the National Spherical Torus Experiment," Phys. Plasmas 19, 056120 (2012).

P A Schneider, E Wolfrum, R J Groebner, T H Osborne, M N A Beurskens, M G Dunne, J R Ferron, S Günter, B Kurzan, K Lackner, P B Snyder, H Zohm, the ASDEX Upgrade Team, the DIII-D Team and JET EFDA Contributors, "Differences in the H-mode Pedestal Width of Temperature and Density," Plasmas Phys. Control. Fusion 54, 105009 (2012).

P.B. Snyder, T.H. Osborne, K.H. Burrell, R.J. Groebner, A.W. Leonard, R. Nazikian, D.M. Orlov, O. Schmitz, M.R. Wade, and H.R. Wilson, "The EPED Pedestal Model and ELM-Suppressed Regimes: Studies of Quiescent H-Mode and Development of a Model for ELM Suppression via Resonant Magnetic Perturbations," Phys. Plasmas **19**, 056115 (2012).

F. Turco, C. T. Holcomb, J. R. Ferron, T. C. Luce, P. A. Politzer, J. M. Park, A. E. White, D. P. Brennan, A. D. Turnbull, J. M. Hanson, M. Okabayashi, and Y. In, "Sensitivity of Transport and Stability to the Current Profile in Steady-State Scenario Plasmas in DIII-D," Phys. Plasmas 19, 122506 (2012).

A.D. Turnbull, "Plasma Response Models for Non-Axisymmetric Perturbations," Nucl. Fusion **52**, 054016 (2012).

J.R. Walk, P.B. Snyder, J.W. Hughes, J.L. Terry, A.E. Hubbard and P.E. Phillips, "Characterization of the Pedestal in Alcator C-Mod ELMing H-Modes and Comparison with the EPED Model," Nucl. Fusion 52, 083001 (2012).

R.E. Waltz and F.L. Waelbroeck, "Gyro-Kinetic Simulations with External Resonant Magnetic Field Perturbations: Island Torque and Non-Ambipolar Transport with Plasma Rotation," Phys. Plasmas **19**, 032508 (2012).

W. Wan, S.E. Parker, Y. Chen, Z. Yan, R.J. Groebner, P.B. Snyder, "Global Gyrokinetic Simulation of Tokamak Edge Plasma Instabilities, " Phys. Rev. Lett. 109, 185004 (2012)

E. Wang, X. Xu, J. Candy, R.J. Groebner, P.B. Snyder, Y. Chen, S.E. Parker, W. Wan, G. Lu, and J.Q. Dong, "Quantitative Comparison of Experimental Impurity Transport with Nonlinear Gyrokinetic Simulation in an Alcator C-Mod L-mode Plasma," Nucl. Fusion 52, 103015 (2012).

GA THEORY PUBLICATIONS FOR 2011

M. Bakhtiari, G. Olynyk, R. Granetz, D.G. Whyte, M.L. Reinke, K. Zhurovich and V. Izzo, "Using Mixed Gases for Massive Gas Injection Disruption Mitigation on Alcator C-Mod," Nucl. Fusion 51, 063007 (2011).

J. A. Baumgaertel, E.A. Belli, W. Dorland, W. Guttenfelder, G.W. Hammett, D.R. Mikkelsen, G. Rewoldt, W.M. Tang, and P. Xanthopoulos, "Simulating Gyrokinetic Microinstabilities in Stellarator Geometry with GS2," Phys. Plasmas 18, 122301 (2011).

E. Belli and J. Candy, "Full Linearized Fokker-Planck Collisions in Neoclassical Transport Simulations," Plasmas Phys. Control. Fusion **54**, 015015 (2011).

M. N. A. Beurskens, T. H. Osborne, P. A. Schneider, E. Wolfrum, L. Frassinetti, R. Groebner, P. Lomas, I. Nunes, S. Saarelma, R. Scannell, P. B. Snyder, D. Zarzoso, I. Balboa, B. Bray, M. Brix, J. Flanagan, C. Giroud, E. Giovannozzi, M. Kempenaars, A. Loarte, E. de la Luna, G. Maddison, C. F. Maggi, D. McDonald, R. Pasqualotto, G. Saibene, R. Sartori, Emilia R. Solano, M. Walsh, L. Zabeo, DIII-D Team, ASDEX Upgrade Team, and JET-EFDA Contributors, "H-mode Pedestal Scaling in DIII-D, ASDEX Upgrade, and JET," Phys. Plasmas 18, 056120 (2011).

J. Boedo, E. Belli, E. Hollmann, W. Solomon, D. Rudakov, J. Watkins, R. Prater, J. Candy, R. Groebner, K. Burrell, C. Lasnier, A. Leonard, R. Moyer, G. Porter, N. Brooks, and E. Unterberg, "Poloidally and Radially Resolved Parallel D^+ Velocity Measurements in the DIII-D Boundary and Comparison to Neoclassical Computations," Phys. Plasmas **18**, 032510 (2011).

D.P. Boyle, R. Maingi, P.B. Snyder, J. Manickam, T.H. Osborne, R.E. Bell, B.P. LeBlanc and the NSTX team, "The Relationships between Edge Localized Modes Suppression, Pedestal Profiles and Lithium Wall Coatings in NSTX," Plasmas Phys. Control. Fusion 53, 105011 (2011).

R.V. Bravenec, J. Candy, M. Barnes, and C. Holland, "Linear and Nonlinear Verification of Gyro-Kinetic Microstability Codes," Phys. Plasmas **18**, 122505 (2011).

N. Commaux, L.R. Baylor, S.K. Combs, N.W. Eidietis, T.E. Evans, C.R. Foust, E.M. Hollmann, D.A. Humphreys, V.A. Izzo, A.N. James, T.C. Jernigan, S.J. Meitner, P.B. Parks, J.C. Wesley and J.H. Yu, "Novel Rapid Shutdown Strategies for Runaway Electron Suppression in DIII-D," Nucl. Fusion 51, 103001 (2011).

J. Candy and E.A. Belli, "Neoclassical Transport Including Collisional Nonlinearity," Phys. Rev. Lett. **106**, 235003 (2011).

V.S. Chan, R.D. Stambaugh, A.M. Garofalo, J. Canik, J.E. Kinsey, J.M. Park, M.Y.K. Peng, T.W. Petrie, M. Porkolab, R. Prater, M. Sawan, J.P. Smith, P.B. Snyder, P.C. Stangeby, and C.P.C. Wong, "A Fusion Development Facility on the Critical Path to Fusion Energy," Nucl. Fusion **51**, 083019 (2011).

M.S. Chu and M. Okabayashi, "Stabilization of the External Kink and Resistive Wall Mode," Plasmas Phys. Control. Fusion **52**, 123001 (2010).

M.S. Chu, L.L. Lao, M.J. Schaffer, T.E. Evans, E.J. Strait, Y.Q. Liu, M.J. Lanctot, H. Reimerdes, Y. Liu, T.A. Casper, and Y. Gribov, "Response of a Resistive and Rotating Tokamak to External Magnetic Perturbations below the Alfvén frequency," Nucl. Fusion **51**, 073036 (2011).

B.D. Dudson, X.Q. Xu, M.V. Umansky, H.R. Wilson, and P.B. Snyder, "Simulation of Edge Localized Modes Using BOUT++," Plasmas Phys. Control. Fusion. **53**, 054005 (2011).

A.R. Field, C. Michael, R.J. Akers, J. Candy, G. Colyer, W. Guttenfelder, Y.-c. Ghim, C.M. Roach, S. Saarelma and the MAST Team, "Plasma Rotation and Transport in MAST Spherical Tokamak," Nucl. Fusion 51, 063006 (2011).

A.M. Garofalo, W.M. Solomon, J.-K. Park, K.H. Burrell, J.C. DeBoo, M.J. Lanctot, G.R. McKee, H. Reimerdes, L. Schmitz, M.J. Schaffer and P.B. Snyder., "Advances Toward QH-mode Viability for ELM-stable Operation in ITER," Nucl. Fusion **51**, 083018 (2011).

W. Guttenfelder and J. Candy, "Resolving electron scale turbulence in spherical tokamaks with flow shear," Phys. Plasmas **18**, 022506 (2011).

T. Hein, C. Angioni, E. Fable, J. Candy, and A. G. Peeters, "Gyrokinetic Study of Electromagnetic Effects on Toroidal Momentum Transport in Tokamak Plasmas," Phys. Plasmas 18, 072503 (2011).

C. Holland, L. Schmitz, T.L. Rhodes, W.A. Peebles, J.C. Hillesheim, G. Wang, L. Zeng, E.J. Doyle, S.P. Smith, R. Prater, K.H. Burrell, J. Candy, R.E. Waltz, J.E. Kinsey, G.M. Staebler, J.C. DeBoo, C.C. Petty, G.R. McKee, Z. Yan, and A.E. White, "Advances in Validating Gyro-Kinetic Turbulence Models against L- and H-Mode Plasmas," Phys. Plasmas **18**, 056113 (2011).

E.M. Hollmann, P.B. Parks, D.A. Humphreys, N.H. Brooks, N. Commaux, N. Eidietis, T.E. Evans, R. Isler, A.N. James, T.C. Jernigan, J. Munoz, E.J. Strait, C. Tsui, J. Wesley and J.H. Yu, "Effect of Applied Toroidal Electric Field on the Growth/Decay of Plateau-Phase Runaway Electron Currents in DIII-D," Nucl. Fusion 51, 103026 (2011).

V.A. Izzo, E.M. Hollmann, A.N. James, J.H. Yu, D.A. Humphrey, L.L. Lao, P.B. Parks, P.E. Sieck, J.C. Wesley, R.S. Granetz, G.M. Olynyz, and D.G. Whyte, "Runaway Electron Confinement Modeling for Rapid Shutdown Scenarios in DIII-D, Alcator C-Mod and ITER," Nucl. Fusion **51**, 063032 (2011).

J.E. Kinsey, G.M. Staebler, J. Candy, R.E. Waltz, and R.V. Budny, "ITER Predictions Using the GYRO Verified and Experimentally Validated TGLF Transport Model," Nucl. Fusion **51**, 083001 (2011).

M. J. Lanctot, H. Reimerdes, A. M. Garofalo, M. S. Chu, J. M. Hanson, Y. Q. Liu, G. A. Navratil, I. N. Bogatu, Y. In, G. L. Jackson, R. J. La Haye, M. Okayabashi, J.-K. Park, M. J. Schaffer, O. Schmitz, E. J. Strait, and A. D. Turnbull, "Measurement and Modeling of Three-Dimensional Equilibria in DIII-D," Phys. Plasmas 18, 056121 (2011).

P. Mantica, C. Angioni, B. Baiocchi, M. Baruzzo, M.N.A Beurskens, J.P.S. Bizarro, R.V. Budny, P. Buratti, A. Casati, C. Challis, J. Citrin, G. Colyer, F. Crisanti, A.C.A. Figueiredo, L. Frassinetti, C. Giroud, N. Hawkes, J. Hobirk, E. Joffrin, T. Johnson, E. Lerche, P. Migliano, V. Naulin, A.G. Peeters, G. Rewoldt, F. Ryter, A. Salmi, R. Sartori, C. Sozzi, G. Staebler, D. Strintzi, T. Tala, M. Tsalas, D. Van Eester, T. Versloot, P.C. deVries, J. Weiland and JET EFDA Contributors, "Ion Heat Transport Studies in JET," Plasmas Phys. Control. Fusion. 53, 124033 (2011).

M. Murakami, J.M. Park, G. Giruzzi, J. Garcia, P. Bonoli, R.V. Budny, E.J. Doyle, A. Fukuyama, N. Hayashi, M. Honda, A. Hubbard, S. Ide, F. Imbeaux, E.F. Jaeger, T.C. Luce, Y.-S. Na, T. Oikawa, T.H. Osborne, V. Parail, A. Polevoi, R. Prater, A.C.C. Sips, J. Snipes, H.E. St. John, P.B. Snyder, I. Voitsekhovitch and ITPA/Integrated Operation Scenario Group, "Integrated Modelling of Steady-State Scenarios and Heating and Current Drive Mixes for ITER," Nucl. Fusion 51, 103006 (2011).

W.M. Nevins, E. Wang, and J. Candy, "Magnetic Stochasticity in Gyrokinetic Simulations of Plasma Microturbulence," Phys. Rev. Lett. **106**, 065003 (2011).

D.C. Pace, R.K. Fisher, M. García-Muñoz, W.W. Heidbrink, G.R. McKee, M. Murakami, C.M. Muscatello, R. Nazikian, J.M. Park, C.C. Petty, T.L. Rhodes, G.M. Staebler, M.A. Van Zeeland, R.E. Waltz, R.B. White, J.H. Yu, W. Zhang and Y.B. Zhu, "Transport of Energetic Ions due to Sawteeth, Alfvén Eigenmodes and Microturbulence," Nucl. Fusion 51, 043012 (2011).

P.B. Parks and W. Wu, "Limitations of Extended Gas Delivery Tubes Used for Fueling Mitigated Plasma Disruptions and a Unique Injection Concept for Prompt Gas Delivery," Nucl. Fusion **51**, 073014 (2011).

T.W. Petrie, T.E. Evans, N.H. Brooks, M.E. Fenstermacher, J.R. Ferron, C.T. Holcomb, B. Hudson, A.W. Hyatt, T.C. Luce, C.J. Lasnier, S. Mordijck, R.A. Moyer, T.H. Osborne, P.A. Politzer, M.E. Rensink, M.J. Schaffer, P.B. Snyder and J.G. Watkins, "Results from Radiating Divertor Experiments with RMP ELM Suppression and Mitigation," Nucl. Fusion 51, 073003 (2011).

I. Pusztai, J. Candy, and P. Gohil, "Isotop Mass and Charge Effects in Tokamak Plasmas," Phys. Plasmas 18, 122501 (2011).

Q. Ren, M.S. Chu, L.L. Lao, and R. Srinivasan, "High Spatial-Resolution Equilibrium Reconstruction and its Force Balance Analysis," Plasmas Phys. Control. Fusion **53**, 095009 (2011).

T.L. Rhodes, C. Holland, S.P. Smith, A.E. White, K.H. Burrell, J. Candy, J.C. DeBoo, E.J. Doyle, J.C. Hillesheim, J.E. Kinsey, G.R. McKee, D. Mikkelsen, W.A. Peebles, C.C. Petty, R. Prater, S. Parker, Y. Chen, L. Schmitz, G.M. Staebler, R.E. Waltz, G. Wang, Z. Yan and L. Zeng, "L-mode Validation Studies of Gyrokinetic Turbulence Simulations via Multiscale and Multifield Turbulence Measurements on the DIII-D Tokamak," Nucl. Fusion 51, 063022 (2011).

P.B. Snyder, R.J. Groebner, J.W. Hughes, T.H. Osborne, M. Buerskens, A.W. Leonard, H.R. Wilson, and X.Q. Xu, "A First Principles Predictive Model of the Pedestal Height and Width: Development, Testing, and ITER Optimization with the EPED Model," Nucl. Fusion **51**, 103016 (2011).

A.C. Sontag, J.M. Canik, R. Maingi, J. Manickam, P.B. Snyder, R.E. Bell, S.P. Gerhardt, S. Kubota, B.P. LeBlanc, D. Mueller, T.H. Osborne and K.L. Tritz, "Pedestal Characterization and Stability of Small-ELM Regimes in NSTX," Nucl. Fusion 51, 103022 (2011).

G.M. Staebler, R.E. Waltz, and J.E. Kinsey "Discoveries from the Exploration of Gyro-Kinetic Momentum Transport," Phys. Plasmas **18**, 056106 (2011).

R.D. Stambaugh, V.S. Chan, A.M. Garofalo, M. Sawan, D.A. Humphreys, L.L. Lao, J.A. Leuer, T.W. Petrie, R. Prater, P.B. Snyder, J.P. Smith, and C.P.C. Wong, "Fusion Nuclear Science Facility Candidates," Fusion Sci. Technol. **59**, 279 (2011).

V. Tangri, P.W. Terry, and R.E. Waltz, "A Circular Equilibrium Model for Local Gyrokinetic Simulations of Ion-Temperature Gradient Fluctuations in Reversed Fuel Pinches," Phys. Plasmas 18, 052310 (2011).

B. J. Tobias, R. L. Boivin, J. E. Boom, I. G. J. Classen, C. W. Domier, A. J. H. Donné, W. W. Heidbrink, N. C. Luhmann, T. Munsat, C. M. Muscatello, R. Nazikian, H. K. Park, D. A. Spong, A. D. Turnbull, M. A. Van Zeeland, G. S. Yun, and DIII-D Team, "On the

Application of Electron Cyclotron Emission Imaging to the Validation of Theoretical Models of Magnetohydrodynamic Activity," Phys. Plasmas 18, 056107 (2011).

A.D. Turnbull, W.A. Cooper, L.L. Lao and Long-Poe Ku, "Ideal MHD Spectrum Calculations for the ARIES-CS Configuration," Nucl. Fusion **51**, 123011 (2011).

M. Valovič, R. Akers, M. de Bock, J. McCone, L. Garzotti, C. Michael, G. Naylor, A. Patel, C.M. Roach, R. Scannell, M. Turnyanskiy, M. Wisse, W. Guttenfelder, J. Candy and the MAST team, "Collisionality and Safety Factor Scalings of H-mode Energy Transport in the MAST Spherical Tokamak," Nucl. Fusion 51, 073045 (2011).

R.E. Waltz, G.M. Staebler, and W. Solomon, "Gyrokinetic Simulation of Momentum Transport with Residual Stress from Diamagnetic Level Velocity Shears," Phys. Plasmas **18**, 042504 (2011).

E. Wang, W.M. Nevins, J. Candy, D. Hatch, P. Terry, and W. Guttenfeider, "Electron Heat Transport from Stochastic Fields in Gyro-Kinetic Simulations," Phys. Plasmas **18**, 056111 (2011).

G. Wang, W. A. Peebles, T. L. Rhodes, J. C. DeBoo, G. M. Staebler, J. C. Hillesheim, Z. Yan, G. R. McKee, C. C. Petty, W. M. Solomon, K. H. Burrell, E. J. Doyle, A. W. Leonard, L. Schmitz, M. A. VanZeeland, A. E. White, and L. Zeng, "Multi-field/Multi-scale Turbulence Response to Electron Cyclotron Heating of DIII-D Ohmic Plasmas," Phys. Plasmas 18, 082504 (2011).

A.E. White, N.T. Howard, D.R. Mikkelsen, M. Greenwald, J. Candy and R.E. Waltz, "Feasibility Study for a Correlation Electron Cyclotron Emission Turbulence Diagnostic Based on Nonlinear Gyrokinetic Simulations," Plasmas Phys. Control. Fusion. 53, 115003 (2011).

S.K. Wong and V.S. Chan, "Numerical Solution of Neoclassical Ion Transport Using Fokker-Planck Operator for Coulomb Collisions," Plasmas Phys. Control. Fusion **53**, 095005 (2011).

X.Q. Xu, B.D. Dudson, P.B. Snyder, M.V. Umansky, H.R. Wilson, and T. Casper, "Nonlinear ELM Simulations Based on a Nonideal Peeling-Ballooning Model Using the BOUT++ Code," Nucl. Fusion **51**, 103040 (2011).

Z. Yan, G. R. McKee, R. J. Groebner, P. B. Snyder, T. H. Osborne, M. N. Beurskens, and K. H. Burrell, "Pedestal Density Fluctuation Dynamics during the Inter-ELM Cycle in DIII-D," Phys. Plasmas 18, 056117 (2011).

ACKNOWLEDGMENT

This work supported by the U.S. Department of Energy under Grant No. DE-FG03-95ER54309.